Title: Recording γ-secretase activity in living mouse brains

Author names and affiliations
Steven S. Hou[#, *], Yuya Ikegawa[#], Yeseo Kwon, Mei C.Q. Houser, Brianna Lundin, Brian J. Bacskai, Oksana Berezovska, and Masato Maesako*

MassGeneral Institute for Neurodegenerative Disease, Massachusetts General Hospital, Harvard Medical School, 114, 16th street, Charlestown, MA 02129

[#] Equally contributed
* Corresponding authors

Corresponding author email address: Steven S. Hou, PhD (shou@mgh.harvard.edu) and Masato Maesako, PhD (MMAESAKO@mgh.harvard.edu)

Abstract
γ-Secretase plays a pivotal role in the central nervous system. Our recent development of genetically encoded Förster resonance energy transfer (FRET)-based biosensors has enabled the spatiotemporal recording of γ-secretase activity on a cell-by-cell basis in live neurons *in culture*. Nevertheless, how γ-secretase activity is regulated *in vivo* remains unclear. Here we employ the near-infrared (NIR) C99 720-670 biosensor and NIR confocal microscopy to quantitatively record γ-secretase activity in individual neurons in living mouse brains. Intriguingly, we uncovered that γ-secretase activity may influence the activity of γ-secretase in neighboring neurons, suggesting a potential "cell non-autonomous" regulation of γ-secretase in mouse brains. Given that γ-secretase plays critical roles in important biological events and various diseases, our new assay *in vivo* would become a new platform that enables dissecting the essential roles of γ-secretase in normal health and diseases.

Introduction
γ-Secretase is an intramembrane aspartyl protease complex responsible for the proteolytic processing of a wide range of transmembrane proteins (Güner and Lichtenthaler, 2020) such as Notch receptors (De Strooper et al., 1998) and APP (De Strooper et al., 1999). γ-Secretase is ubiquitously expressed in various tissues and plays multifunctional roles in essential biology and diseases. For instance, the mice lacking presenilin (PSEN) 1 and 2, the catalytic component of γ-secretase (Wolfe et al., 1999), are nonviable due to abnormal neurogenesis and vasculature and skeletal formation (Shen et al., 1997; Wong et al., 1997). Notch knockout (KO) mice recapitulate the lethal phenotypes of the PSEN1/2 KO (Swiatek et al., 1994; Huppert et al., 2000), suggesting the essential role of γ-secretase-mediated Notch processing in normal development. Aberrant Notch processing also causes several types of cancer (Allenspach et al., 2002; Aster et al., 2017; McCaw et al., 2021) as well as a chronic skin inflammatory disease - Hidradenitis suppurativa (HS) (Wang et al., 2010; Wang et al., 2020).

γ-Secretase plays an essential role in the central nervous system. Conditional knockout of PSEN1 and 2 (Saura et al., 2004) or other components of γ-secretase in excitatory (Tabuchi et al., 2009; Acx et al., 2017; Bi et al., 2021), as well as inhibitory neurons (Kang and Shen, 2020), leads to age-dependent neuronal loss in adult mice. Mutations in PSEN genes lead to early-onset familial Alzheimer's disease (AD) (Sherrington et al., 1995; Levy-Lahad et al., 1995) and frontotemporal dementia (FTD) (Raux et al., 2000; Dermaut et al., 2004). Some PSEN mutations are linked to epilepsy (Mann et al., 2001; Velez-Pardo et al., 2004). γ-Secretase is also responsible for the generation of β-amyloid (Aβ) peptides (De Strooper et al., 1999), the accumulation of which in the brain parenchyma is one of the pathological hallmarks of AD. Altogether, it is highly plausible that changes in γ-secretase activity could be ultimately linked to the development and progression of neurodegenerative diseases such as AD.

Our recent development of the genetically encoded C99 YPet-TurquoiseGL (C99 Y-T) biosensor has, for the first time, allowed recording γ-secretase activity over time, on a cell-by-cell basis, in live neurons *in culture*. Using the C99 Y-T biosensor, we uncovered that γ-secretase activity is heterogeneously regulated among mouse cortex primary neurons (Maesako et al., 2020). Nevertheless, to investigate the role of γ-secretase in-

depth, an assay that permits the investigation of the dynamics of γ-secretase in more physiological conditions *in vivo* would be required. In the conventional γ-secretase activity assay, APP or Notch1-based recombinant substrates and isolated γ-secretase-rich membrane fractions from rodent/human brains are incubated *in vitro*, followed by the detection of either Aβ peptides or the intracellular domain fragment (Hoke et al., 2005; Kakuda et al., 2006; Szaruga et al., 2015). Though the assay is highly sensitive, it only reports γ-secretase activity in a bulk population of cells *ex vivo*, and neither provides spatiotemporal nor cell-by-cell information about the γ-secretase activity in live cells *in vivo*.

In order to overcome these critical shortcomings and fulfill the detection capability of γ-secretase activity *in vivo*, we have recently developed a near-infrared (NIR) analog: C99 720-670 biosensor and validated the reporter probe *in culture* (Houser et al., 2020), since the NIR spectral region exhibits greater depth penetration and minimal absorption, and this spectral region exhibits low autofluorescence. In this study, we employed AAV delivery of the C99 720-670 biosensor and NIR confocal microscopy to monitor γ-secretase activity in intact mouse brains. This study, for the first time, reports successful recording of γ-secretase activity on a cell-by-cell basis in live neurons *in vivo,* as opposed to an existing assay in a bulk population of cells *ex vivo*. Moreover, it highlights the feasibility of NIR confocal microscopy for monitoring biological events in live mouse brains. In agreement with the previous study *in vitro*, we uncovered that γ-secretase activity is differently regulated in individual neurons in live mouse brains *in vivo*. Although the effect size is modest, we also found a statistically significant correlation between γ-secretase activity within a neuron and the activity of γ-secretase in neighboring neurons, suggesting a potential “cell non-autonomous” regulation of γ-secretase activity in mouse brains. The new *in vivo* imaging platform would help to better understand the spatiotemporal regulation of γ-secretase and its consequences in normal health and disease-relevant conditions.

Materials and Methods

Ethics

Experimental procedures were in compliance with the NIH guidelines for the use of animals in experiments and were approved by the Massachusetts General Hospital Animal Care and Use Committee (2003N000243).

Adeno-associated virus (AAV)

Preparation of the AAV-hSyn1-C99 720-670 was performed as described previously (Maesako et al., 2022). Briefly, the cDNA of the C99 720-670 biosensor (Houser et al., 2020) was sub-cloned into a pAAV vector containing human Synapsin 1 promoter and WPRE sequences (Maesako et al., 2017). The plasmid sequence was verified by the MGH DNA core. The packaging into viruses (AAV2/8 stereotype) was performed at the University of Pennsylvania Gene Therapy Program vector core (Philadelphia, PA) (4.95E+13 GC/mL). The AAV-hSyn1-C99 720-670 was injected into the somatosensory cortex of 4-6 months old C57BL/6 male mice.

Craniotomy

Craniotomy surgery was performed based on previously described methods (Kuchibhotla et al., 2008) with minor adjustments. Briefly, C57BL/6 mice were anesthetized using 1-1.5% isoflurane. A ~3.5 mm circular section of the skull over the right hemisphere of the brain was surgically removed. The dura mater was left intact during the craniotomy procedure. A 4 mm cover glass was then positioned over the exposed brain area and secured with a mixture of dental acrylic and cyanoacrylate glue. Post-surgery, mice received buprenorphine and Tylenol for pain relief over 3 days. The mice were left to recover for at least 3 weeks before proceeding with the imaging experiments.

NIR confocal microscopy

A diode laser at 640 nm wavelengths was used to excite the C99 720-670 biosensor. Fluorescence emission from miRFP670 (donor) and miRFP720 (acceptor) in the detection range: 670 ± 10 nm and 750 ± 50 nm, respectively, was detected by the high sensitivity-spectral detector, equipping cooled GaAsP photomultiplier on an Olympus FV3000RS confocal microscope. A x25 objective (NA = 1.05) was used for the image acquisition (512 x 512 pixels, Zoom x1). To obtain Z-stack images, the image acquisition was started at the first appearance of vasculature near the brain surface and continued at 2 μm step sizes up to approximately 60-80 sections.

Image processing, quantification, and statistical analysis

For quantification, the 3D ImageJ Suite plugin (Ollion et al., 2013) in Fiji was used to automatically segment neurons expressing the C99 720-670 biosensor. In image processing, top-hat filtering was first applied to remove uneven background illumination (filter size: r = 7) as described previously (Netten et al., 1997; Gué et al., 2005). Then, median filtering was used to remove noise from the images (filter size: r = 3) (Huang et al., 1979). After the removal of the background and noise, 3D iterative thresholding (Gul-Mohammed et al., 2014) using the MSER criteria (Matas et al., 2004) was adapted to draw ROIs on the neuronal cell bodies (300-10000 voxels). Lastly, the morphological opening operation was applied to remove wrongly assigned ROIs (filter size: r = 2) (Meyer and Beucher, 1990). In order to determine γ-secretase activity on a cell-by-cell basis, the donor (miRFP670) and acceptor (miRFP720) fluorescence intensities in ROIs were measured, and the acceptor over donor emission ratios (i.e., 720/670 ratios) were calculated. Then, the distance between an ROI and other ROIs was measured using Scikit-learn (Pedregosa et al., 2012) in Python, which was used to identify neighboring neurons (e.g., 2, 5, 10 closest neurons, neurons within a 20 μm radius). In the statistical analysis, the Pearson correlation coefficient was measured to determine if the 720/670 ratios in a neuron significantly correlate with the 720/670 ratios of neighboring neurons, which was performed using Scipy (Virtanen et al., 2020) in Python. $P < 0.05$ was considered statistically significant. The sample size was calculated based on previous correlation analysis in our *in vitro* studies (Houser et al., 2021; Maesako et al., 2022) and was estimated to include approximately n = 200 - 250 neurons/region-of-interests (ROIs) per animal. Pseudo-color images corresponding to the 720/670 ratios were generated in MATLAB (MathWorks, Natick, MA).

Results

Expression of the C99 720-670 biosensor in the somatosensory cortex of live mice

We have recently developed genetically encoded FRET-based biosensors that, for the first time, allow quantitative recording of γ-secretase activity on a cell-by-cell basis in cultured neurons (Maesako et al., 2020; Houser et al., 2020). The principle of the biosensors is that the C-terminus of APP C99, an immediate substrate of γ-secretase, is fused to the FRET donor and acceptor fluorescent proteins with a flexible linker, and the sensing domains are stabilized near the membrane by connecting to a membrane-anchoring domain. The proteolytic processing of C99 within the biosensor by endogenous γ-secretase results in a change in the proximity and/or orientation between the donor and acceptor fluorophores, which can be recorded as altered FRET efficiency (**Fig. 1A**). Of note, we ensured that the fusion of the donor/acceptor fluorescent proteins and the anchor domain does not significantly affect the cleavage efficiency of C99 by γ-secretase by evaluating the processing efficiency between the cells expressing C99 FLAG and our FRET probe (Maesako et al., 2020; Houser et al., 2020). To elucidate the cell-by-cell regulation of γ-secretase activity in live mouse brains *in vivo*, we administrated an AAV that packages the C99 720-670 biosensor into the somatosensory cortex of 4-6 months old C57BL/6 mice implanted with cranial window for imaging (**Fig. 1B**). 3-4 weeks post AAV injection, we successfully detected the neurons expressing the C99 720-670 sensor using a confocal microscope with single-photon excitation at 640 nm wavelength and emission at 700-800 nm range (**Fig. 1C** and **D**). Notably, the fluorescence signal from the C99 720-670 biosensor could be detected from the brain surface to approximately 100 μm depth (**Fig. 2**).

Automatic segmentation of neurons expressing the C99 720-670 biosensor

In image processing (**Fig. 3A**), the background fluorescence was first subtracted, and the noise was reduced in the images using median filtering to perform the automatic segmentation of individual neurons. Then, an initial set of ROIs was automatically created on all cellular structures in the images using 3D iterative thresholding. Next, the intensities of the donor (miRFP670) and acceptor (miRFP720) fluorescence were measured, and the acceptor over donor emission ratios (i.e., 720/670 ratios) were calculated for each ROI. Of note, we uncovered that those ROIs contained non-specific autofluorescent objects whose morphology clearly differed from neurons (**Fig. 4A**). Therefore, morphological filtering was first applied to exclude the non-specific objects from ROIs. Moreover, we analyzed the scatter plot of 720/670 ratios (Y-axis: miRFP670 emission, X-axis: miRFP720 emission) and found that the autofluorescent objects have a significantly lower 720/670 ratio compared to neurons expressing C99 720-670 (**Fig. 4B**). We also confirmed the identity of the autofluorescent objects by imaging using the same microscope settings in mice without AAV-hSyn1-C99 720-670 injection and found the same population of non-specific objects with low 720/670 ratios is present. Therefore, in the segmentation procedure, we excluded the ROIs exhibiting 720/670 ratios below a set threshold value as 1.5.

"Cell non-autonomous" regulation of γ-secretase in mouse brains

To elucidate how the γ-secretase activity is regulated on a cell-by-cell basis *in vivo*, we first measured the distance between pairs of neurons, then identified each neuron's five closest neurons, and calculated the average 720/670 ratio of the five neighboring neurons. Then, the Pearson correlation coefficient was measured to determine if there is a linear correlation between the 720/670 ratio (as a measure of γ-secretase activity) in each neuron and the average ratio of the five neighboring neurons (**Fig. 3B**). Intriguingly, we found that neighboring neurons likely exhibited similar 720/670 ratios (i.e., "clustering" of the neurons displaying similar 720/670 ratios) (**Fig. 5A**). Indeed, while the effect is modest, unbiased quantification and statistical analysis showed a significant linear correlation between the 720/670 ratio in each neuron and the average ratio in five neighboring neurons (**Fig. 5B**). Such a statistically significant positive correlation was also detected in two other mice (**Fig. 5C** and **5D**), suggesting that γ-secretase activity in a neuron may positively correlate with the degree of activity in its neighboring neurons. We also ensured that the 720/670 ratio was positively correlated with the average 720/670 ratio of the two and ten neighboring neurons (**Fig. 6A-C**). To further corroborate these findings, we determined the average 720/670 ratio of neurons within a 20 μm radius and examined the correlation between the 720/670 ratio in each neuron and the average 720/670 ratio in neighboring neurons (**Fig. 7A**). We found a significant linear correlation between the 720/670 ratio in each neuron and the average ratio of neurons within 20 μm radius in three independent mice (**Fig. 7B-D**), further evidencing neurons displaying similar 720/670 ratios co-localize in mouse brains. Furthermore, we examined if inhibition of γ-secretase can cancel the clustering of the neurons exhibiting similar levels of γ-secretase activities. As such, we subcutaneously administrated a potent γ-secretase inhibitor: DAPT (Dovey et al., 2001). We found that DAPT dose-dependently increased APP C-terminal fragments (APP CTFs), immediate substrates of γ-secretase. In contrast, full-length APP levels were not significantly altered (**Fig. 8A**), suggesting that DAPT inhibits γ-secretase in the brain. Then, we administrated 100 mg/kg DAPT into mice expressing the C99 720-670 biosensor, performed confocal microscopy, adapted the same imaging processing, and performed correlation analysis between the 720/670 ratio in each neuron and the average ratio of the five neighboring neurons or the neurons within 20 μm radius. Notably, there was no significant correlation in DAPT-administrated mice (**Fig. 8B-E**), suggesting that the positive correlation between the 720/670 ratio in each neuron and the average ratio in neighboring neurons is canceled by the inhibition of γ-secretase and thus the positive correlation is dependent on γ-secretase activity. Collectively, these results strongly indicate that γ-secretase activities are synchronized in neighboring neurons, and γ-secretase activity may be "cell non-autonomously" regulated in living mouse brains.

Discussion

The brain is one of the tissues in which γ-secretase complexes play vital roles. For example, γ-secretase generates Aβ peptides (De Strooper et al., 1999), which are accumulated in AD brains. Recent clinical trials show that antibodies against Aβ can slow cognitive decline in AD (van Dyck et al., 2023; Sims et al., 2023). Moreover, γ-secretase is also responsible for maintaining neuronal survival (Saura et al., 2004; Tabuchi et al., 2009; Acx et al., 2017; Bi et al., 2021). However, little is known about how endogenous γ-secretase activity is spatiotemporally regulated in the intact brain. In the present study, we recorded γ-secretase activity in individual neurons in a living mouse brain by employing AAV-mediated gene delivery to express the NIR range γ-secretase reporter: C99 720-670 biosensor (Houser et al., 2020). Using NIR confocal microscopy, we uncovered that γ-secretase activity influences the activity of γ-secretase in neighboring neurons, suggesting a potential "cell non-autonomous" regulation of γ-secretase in mouse brains.

Whether the γ-secretase activity is similarly or differently regulated among neurons remains elusive. A previous study employing microengraving technology reported that individual neurons generate and secrete different levels of Aβ peptides (Liao et al., 2016). In the same line, our FRET-based biosensors have allowed "visualizing" that γ-secretase activity is heterogeneously regulated on a cell-by-cell basis in primary neurons (Maesako et al., 2020). Furthermore, the cell-by-cell heterogeneity in γ-secretase activity was further verified using 1) unique multiplexing FRET analysis in which the processing of two different substrates (e.g., APP vs. Notch1) by γ-secretase can be simultaneously measured in the same cell (Houser et al., 2021), and 2) multiplexed immunocytochemistry in which intracellular Aβ is detected on a cell-by-cell basis (McKendell et al., 2022). Our new study further adds that each neuron exhibits a distinct level of γ-secretase activity in intact mouse brains.

Although increasing evidence suggests γ-secretase activity is heterogeneously regulated on a cell-by-cell basis, little is known about the molecular mechanism(s) underlying such heterogeneity. Given that there are two isoforms of PSEN (i.e., PSEN1 and PSEN2) and three Aph1 (Aph1a, Aph1b, and Aph1c) in rodents, six different γ-secretase complexes can be expressed by the same cells. While the PSEN1 knockout mice displayed a lethal phenotype (Shen et al., 1997; Wong et al., 1997), the PSEN2 knockout revealed no severe phenotypes (Herreman et al., 1999). Furthermore, Aph1a knockout mice show a lethal phenotype, whereas those lacking Aph1b or Aph1c survive into adulthood (Serneels et al., 2005). These studies suggest that different γ-secretase complexes exhibit distinct γ-secretase activity. In this sense, the spatiotemporal expression of different γ-secretase complexes could explain the cell-by-cell basis heterogeneity in γ-secretase activity. On the other hand, previous studies utilizing pharmacological agents that bind to the active form of γ-secretase demonstrated that only a small portion of PSEN might be engaged in the active γ-secretase complex (Lai et al., 2003; Placanica et al., 2009). If this is the case, different equilibrium between the active and inactive γ-secretase could be another possible explanation of the heterogeneity in cellular γ-secretase activity.

Interestingly, we also uncovered not drastic but a statistically significant positive correlation between the 720/670 ratio and those ratios in neighboring neurons (**Fig. 5-7**), suggesting that neurons with similar levels of γ-secretase activity form a cluster. Of note, this positive correlation in the γ-secretase activities is canceled by pharmacological inhibition of γ-secretase (**Fig. 8**). Although these results implicate that γ-secretase activity "propagates" from neuron to neuron, the underlying mechanism remains elusive. Interestingly, a recent study shows that Aβ42 exerts product feedback inhibition on γ-secretase (Zoltowska et al., 2023), suggesting that secreted Aβ42 may be one of the negative regulators of γ-secretase. Furthermore, it is reported that hypoxia-inducible factor-1 alpha (HIF-1α), which is activated under hypoxia (Semenza et al., 1991; Semenza et al., 1992), regulates γ-secretase activity (Villa et al., 2014; Alexander et al., 2022). Therefore, local oxygen concentration may be linked to the clustering of neurons exhibiting similar levels of γ-secretase activity.

Conditional knockout of γ-secretase in the adult neurons displays synaptic dysfunctions, neuroinflammation, and neuronal loss in an age-dependent manner (Saura et al., 2004; Tabuchi et al., 2009; Acx et al., 2017; Bi et al., 2021). It is plausible that γ-secretase may function as "a membrane proteasome" (Kopan and Ilagan, 2004), responsible for the degradation of over 150 different substrate stubs to maintain proper membrane homeostasis, which may be critical for neuronal survival. Notably, a conditional knockout strategy has also elucidated the critical roles of γ-secretase beyond the CNS, i.e., in other tissues, *in vivo*. For instance, specific PSEN1 knockout in hematopoietic progenitors demonstrated the importance of PSEN1/γ-secretase in developing and sustaining leukemia (Habets et al., 2019). Although GSIs were discontinued in the clinical trials of AD, their inhibiting effects on Notch signaling have led to the repurposing of GSIs as anticancer drugs (reviewed in McCaw et al., 2021). Furthermore, epidermis-specific Nicastrin conditional knockout allowed the identification of IL-36a as a key inflammatory cytokine involved in the malfunction of the skin barrier in the pathogenesis of HS (Yang et al., 2020). However, it is difficult to determine by existing tools how endogenous γ-secretase activity is spatiotemporally regulated and how the altered γ-secretase activity contributes to the disease progression. These dynamic processes in living cells can be directly monitored using our FRET-based imaging assays.

In conclusion, this study provides a new imaging prototype to better understand the regulation of γ-secretase and its consequences in living mice *in vivo*. We have recorded γ-secretase activity on a cell-by-cell basis in mouse brains and found that neighboring neurons exhibit similar levels of γ-secretase activity, suggesting that γ-secretase influences the activity of γ-secretase in surrounding neurons.

Conflict of interest statement

The authors declare no conflicts of interest with the contents of this article.

Acknowledgments

This work was funded by the National Institute of Health grants AG79838 (M.M.)

References

Acx H, Serneels L, Radaelli E, Muyldermans S, Vincke C, Pepermans E, Müller U, Chávez-Gutiérrez L, De Strooper B. Inactivation of γ-secretases leads to accumulation of substrates and non-Alzheimer neurodegeneration. EMBO Mol Med. 2017 Aug;9(8):1088-1099.

Alexander C, Li T, Hattori Y, Chiu D, Frost GR, Jonas L, Liu C, Anderson CJ, Wong E, Park L, Iadecola C, Li YM. Hypoxia Inducible Factor-1α binds and activates γ-secretase for Aβ production under hypoxia and cerebral hypoperfusion. Mol Psychiatry. 2022 Oct;27(10):4264-4273.

Allenspach EJ, Maillard I, Aster JC, Pear WS. Notch signaling in cancer. Cancer Biol Ther. 2002 Sep-Oct;1(5):466-76

Aster JC, Pear WS, Blacklow SC. The Varied Roles of Notch in Cancer. Annu Rev Pathol. 2017 Jan 24;12:245-275.

Bi HR, Zhou CH, Zhang YZ, Cai XD, Ji MH, Yang JJ, Chen GQ, Hu YM. Neuron-specific deletion of presenilin enhancer2 causes progressive astrogliosis and age-related neurodegeneration in the cortex independent of the Notch signaling. CNS Neurosci Ther. 2021 Feb;27(2):174-185

Dermaut, B.; Kumar-Singh, S.; Engelborghs, S.; Theuns, J.; Rademakers, R.; Saerens, J.; Pickut, B.A.; Peeters, K.; van den Broeck, M.; Vennekens, K.; et al. A novel presenilin 1 mutation associated with Pick's disease but not beta-amyloid plaques. Ann. Neurol. 2004, 55, 617–626.

De Strooper, B.; Saftig, P.; Craessaerts, K.; Vanderstichele, H.; Guhde, G.; Annaert,W.; Von Figura, K.; Van Leuven, F. Deficiency of presenilin-1 inhibits the normal cleavage of amyloid precursor protein. Nature 1998, 391, 387–390.

De Strooper, B.; Annaert, W.; Cupers, P.; Saftig, P.; Craessaerts, K.; Mumm, J.S.; Schroeter, E.H.; Schrijvers, V.; Wolfe, M.S.; Ray,W.J.; et al. A presenilin-1-dependent gamma-secretase-like protease mediates release of Notch intracellular domain. Nature 1999, 398, 518–522.

Dovey HF, John V, Anderson JP, Chen LZ, de Saint Andrieu P, Fang LY, Freedman SB, Folmer B, Goldbach E, Holsztynska EJ, Hu KL, Johnson-Wood KL, Kennedy SL, Kholodenko D, Knops JE, Latimer LH, Lee M, Liao Z, Lieberburg IM, Motter RN, Mutter LC, Nietz J, Quinn KP, Sacchi KL, Seubert PA, Shopp GM, Thorsett ED, Tung JS, Wu J, Yang S, Yin CT, Schenk DB, May PC, Altstiel LD, Bender MH, Boggs LN, Britton TC, Clemens JC, Czilli DL, Dieckman-McGinty DK, Droste JJ, Fuson KS, Gitter BD, Hyslop PA, Johnstone EM, Li WY, Little SP, Mabry TE, Miller FD, Audia JE. Functional gamma-secretase inhibitors reduce beta-amyloid peptide levels in brain. J Neurochem. 2001 Jan;76(1):173-81.

Gué, Michael, Cédric Messaoudi, Jian Sheng Sun, and Thomas Boudier. 2005. "Smart 3D-FISH: Automation of Distance Analysis in Nuclei of Interphase Cells by Image Processing." Cytometry. Part A: The Journal of the International Society for Analytical Cytology 67 (1): 18–26.

Gul-Mohammed, Jaza, Ignacio Arganda-Carreras, Philippe Andrey, Vincent Galy, and Thomas Boudier. 2014. "A Generic Classification-Based Method for Segmentation of Nuclei in 3D Images of Early Embryos." BMC Bioinformatics 15 (1): 1–12.

Güner, G.; Lichtenthaler, S.F. The substrate repertoire of g-secretase/presenilin. Semin. Cell Dev. Biol. 2020,105, 27–42.

Habets RA, de Bock CE, Serneels L, Lodewijckx I, Verbeke D, Nittner D, Narlawar R, Demeyer S, Dooley J, Liston A, Taghon T, Cools J, de Strooper B. Safe targeting of T cell acute lymphoblastic leukemia by pathology-specific NOTCH inhibition. Sci Transl Med. 2019 May 29;11(494):eaau6246.

Herreman A, Hartmann D, Annaert W, Saftig P, Craessaerts K, Serneels L, Umans L, Schrijvers V, Checler F, Vanderstichele H, Baekelandt V, Dressel R, Cupers P, Huylebroeck D, Zwijsen A, Van Leuven F, De Strooper

B. Presenilin 2 deficiency causes a mild pulmonary phenotype and no changes in amyloid precursor protein processing but enhances the embryonic lethal phenotype of presenilin 1 deficiency. Proc Natl Acad Sci U S A. 1999 Oct 12;96(21):11872-7.

Hoke DE, Tan JL, Ilaya NT, Culvenor JG, Smith SJ, White AR, Masters CL, Evin GM. In vitro gamma-secretase cleavage of the Alzheimer's amyloid precursor protein correlates to a subset of presenilin complexes and is inhibited by zinc. FEBS J. 2005 Nov;272(21):5544-57.

Houser, MCQ.; Hou, SS.; Perrin, F.; Turchyna, Y.; Bacskai, BJ.; Berezovska, O.; Maesako, M. A novel NIR FRET biosensor for reporting PS/γ-secretase activity in living cells. Sensors. 2020 20, 5980

Houser MCQ, Turchyna Y, Perrin F, Chibnik L, Berezovska O, Maesako M. Limited Substrate Specificity of PS/γ-Secretase Is Supported by Novel Multiplexed FRET Analysis in Live Cells. Biosensors (Basel). 2021 May 26;11(6):169.

Huang, T., G. Yang, and G. Tang. 1979. “A Fast Two-Dimensional Median Filtering Algorithm.” IEEE Transactions on Acoustics, Speech, and Signal Processing 27 (1): 13–18.

Huppert SS.; Le A.; Schroeter EH.; Mumm JS.; Saxena MT.; Milner LA.; Kopan R. Embryonic lethality in mice homozygous for a processing-deficient allele of Notch1. Nature. 2000 Jun 22;405(6789):966-70.

Kakuda N, Funamoto S, Yagishita S, Takami M, Osawa S, Dohmae N, Ihara Y. Equimolar production of amyloid beta-protein and amyloid precursor protein intracellular domain from beta-carboxyl-terminal fragment by gamma-secretase. J Biol Chem. 2006 May 26;281(21):14776-86.

Kang J, Shen J. Cell-autonomous role of Presenilin in age-dependent survival of cortical interneurons. Mol Neurodegener. 2020 Dec 10;15(1):72.

Kopan R, Ilagan MX. Gamma-secretase: proteasome of the membrane? Nat Rev Mol Cell Biol. 2004 Jun;5(6):499-504

Kuchibhotla KV, Goldman ST, Lattarulo CR, Wu HY, Hyman BT, Bacskai BJ. Aβ plaques lead to aberrant regulation of calcium homeostasis in vivo resulting in structural and functional disruption of neuronal networks. Neuron. 2008 Jul 31;59(2):214-25.

Lai MT, Chen E, Crouthamel MC, DiMuzio-Mower J, Xu M, Huang Q, Price E, Register RB, Shi XP, Donoviel DB, Bernstein A, Hazuda D, Gardell SJ, Li YM. Presenilin-1 and presenilin-2 exhibit distinct yet overlapping gamma-secretase activities. J Biol Chem. 2003 Jun 20;278(25):22475-81.

Levy-Lahad, E.;Wasco,W.; Poorkaj, P.; Romano, D.M.; Oshima, J.; Pettingell,W.H.; Yu, C.E.; Jondro, P.D.; Schmidt, S.D.; Wang, K.; et al. Candidate gene for the chromosome 1 familial Alzheimer’s disease locus. Science 1995, 269, 973–977.

Liao MC, Muratore CR, Gierahn TM, Sullivan SE, Srikanth P, De Jager PL, Love JC, Young-Pearse TL. Single-Cell Detection of Secreted Aβ and sAPPα from Human IPSC-Derived Neurons and Astrocytes. J Neurosci. 2016 Feb 3;36(5):1730-46.

Maesako M, Horlacher J, Zoltowska KM, Kastanenka KV, Kara E, Svirsky S, Keller LJ, Li X, Hyman BT, Bacskai BJ, Berezovska O. Pathogenic PS1 phosphorylation at Ser367. Elife. 2017 Jan 30;6:e19720.

Maesako, M.; Sekula, NM.; Aristarkhova, A.; Feschenko, P.; Anderson, LC.; Berezovska, O. Visualization of PS/γ-Secretase Activity in Living Cells. iScience. 2020 May 7;23(6):101139.

Maesako M, Houser MCQ, Turchyna Y, Wolfe MS, Berezovska O. Presenilin/γ-Secretase Activity Is Located in Acidic Compartments of Live Neurons. J Neurosci. 2022 Jan 5;42(1):145-154.

Mann DMA, Pickering Brown SM, Takeuchi A, Iwatsubo T, the members of the Familial Alzheimer's Disease Pathology Study Group. Amyloid angiopathy and variability in amyloid β deposition is determined by mutation position in presenilin-1-linked Alzheimer's disease. Am J Pathol 2001;158:2165–75.

Matas, J., O. Chum, M. Urban, and T. Pajdla. 2004. “Robust Wide-Baseline Stereo from Maximally Stable Extremal Regions.” Image and Vision Computing 22 (10): 761–67.

McCaw TR, Inga E, Chen H, Jaskula-Sztul R, Dudeja V, Bibb JA, Ren B, Rose JB. Gamma Secretase Inhibitors in Cancer: A Current Perspective on Clinical Performance. Oncologist. 2021 Apr;26(4):e608-e621.

McKendell AK, Houser MCQ, Mitchell SPC, Wolfe MS, Berezovska O, Maesako M. In-Depth Characterization of Endo-Lysosomal Aβ in Intact Neurons. Biosensors (Basel). 2022 Aug 20;12(8):663.

Meyer, F., and S. Beucher. 1990. “Morphological Segmentation.” Journal of Visual Communication and Image Representation 1 (1): 21–46.

Netten, H., I. T. Young, L. J. van Vliet, H. J. Tanke, H. Vroljik, and W. C. Sloos. 1997. “FISH and Chips: Automation of Fluorescent Dot Counting in Interphase Cell Nuclei.” Cytometry 28 (1): 1–10.

Ollion J, Cochennec J, Loll F, Escudé C, Boudier T. TANGO: a generic tool for high-throughput 3D image analysis for studying nuclear organization. Bioinformatics. 2013 Jul 15;29(14):1840-1.

Pedregosa, Fabian, Gaël Varoquaux, Alexandre Gramfort, Vincent Michel, Bertrand Thirion, Olivier Grisel, Mathieu Blondel, et al. 2012. “Scikit-Learn: Machine Learning in Python.” ArXiv [Cs.LG]. arXiv. https://www.jmlr.org/papers/volume12/pedregosa11a/pedregosa11a.pdf?ref=https:/.

Placanica L, Tarassishin L, Yang G, Peethumnongsin E, Kim SH, Zheng H, Sisodia SS, Li YM. Pen2 and presenilin-1 modulate the dynamic equilibrium of presenilin-1 and presenilin-2 gamma-secretase complexes. J Biol Chem. 2009 Jan 30;284(5):2967-2977.

Raux, G.; Gantier, R.; Thomas-Anterion, C.; Boulliat, J.; Verpillat, P.; Hannequin, D.; Brice, A.; Frebourg, T.; Campion, D. Dementia with prominent frontotemporal features associated with L113P presenilin 1 mutation. Neurology 2000, 55, 1577–1578.

Saura CA, Choi SY, Beglopoulos V, Malkani S, Zhang D, Shankaranarayana Rao BS, Chattarji S, Kelleher RJ 3rd, Kandel ER, Duff K, Kirkwood A, Shen J. Loss of presenilin function causes impairments of memory and synaptic plasticity followed by age-dependent neurodegeneration. Neuron. 2004 Apr 8;42(1):23-36.

Semenza GL, Koury ST, Nejfelt MK, Gearhart JD, Antonarakis SE. Cell-type-specific and hypoxia-inducible expression of the human erythropoietin gene in transgenic mice. Proc Natl Acad Sci U S A. 1991 Oct 1;88(19):8725-9.

Semenza GL, Wang GL. A nuclear factor induced by hypoxia via de novo protein synthesis binds to the human erythropoietin gene enhancer at a site required for transcriptional activation. Mol Cell Biol. 1992 Dec;12(12):5447-54.

Serneels L, Dejaegere T, Craessaerts K, Horré K, Jorissen E, Tousseyn T, Hébert S, Coolen M, Martens G, Zwijsen A, Annaert W, Hartmann D, De Strooper B. Differential contribution of the three Aph1 genes to gamma-secretase activity in vivo. Proc Natl Acad Sci U S A. 2005 Feb 1;102(5):1719-24.

Shen, J.; Bronson, R.T.; Chen, D.F.; Xia, W.; Selkoe, D.J.; Tonegawa, S. Skeletal and CNS defects in Presenilin-1-deficient mice. Cell 1997, 89, 629–639.

Sherrington, R.; Rogaev, E.I.; Liang, Y.; Rogaeva, E.A.; Levesque, G.; Ikeda, M.; Chi, H.; Lin, C.; Li, G.; Holman, K.; et al. Cloning of a gene bearing missense mutations in early-onset familial Alzheimer’s disease. Nature 1995, 375, 754–760.

Sims JR, Zimmer JA, Evans CD, Lu M, Ardayfio P, Sparks J, Wessels AM, Shcherbinin S, Wang H, Monkul Nery ES, Collins EC, Solomon P, Salloway S, Apostolova LG, Hansson O, Ritchie C, Brooks DA, Mintun M, Skovronsky DM; TRAILBLAZER-ALZ 2 Investigators. Donanemab in Early Symptomatic Alzheimer Disease: The TRAILBLAZER-ALZ 2 Randomized Clinical Trial. JAMA. 2023 Aug 8;330(6):512-527.

Swiatek PJ, Lindsell CE, del Amo FF, Weinmaster G, Gridley T. Notch1 is essential for postimplantation development in mice. Genes Dev. 1994 Mar 15;8(6):707-19.

Szaruga M, Veugelen S, Benurwar M, Lismont S, Sepulveda-Falla D, Lleo A, Ryan NS, Lashley T, Fox NC, Murayama S, Gijsen H, De Strooper B, Chávez-Gutiérrez L. Qualitative changes in human γ-secretase underlie familial Alzheimer's disease. J Exp Med. 2015 Nov 16;212(12):2003-13.

Tabuchi K, Chen G, Südhof TC, Shen J. Conditional forebrain inactivation of nicastrin causes progressive memory impairment and age-related neurodegeneration. J Neurosci. 2009 Jun 3;29(22):7290-301.

van Dyck CH, Swanson CJ, Aisen P, Bateman RJ, Chen C, Gee M, Kanekiyo M, Li D, Reyderman L, Cohen S, Froelich L, Katayama S, Sabbagh M, Vellas B, Watson D, Dhadda S, Irizarry M, Kramer LD, Iwatsubo T. Lecanemab in Early Alzheimer's Disease. N Engl J Med. 2023 Jan 5;388(1):9-21.

Velez-Pardo C, Arellano JI, Cardona-Gomez P, et al. CA1 hippocampal neuronal loss in familial Alzheimer's disease presenilin-1 E280A mutation is related to epilepsy. Epilepsia 2004, 45:751–6.

Villa JC, Chiu D, Brandes AH, Escorcia FE, Villa CH, Maguire WF, Hu CJ, de Stanchina E, Simon MC, Sisodia SS, Scheinberg DA, Li YM. Nontranscriptional role of Hif-1α in activation of γ-secretase and notch signaling in breast cancer. Cell Rep. 2014 Aug 21;8(4):1077-92.

Virtanen, Pauli, Ralf Gommers, Travis E. Oliphant, Matt Haberland, Tyler Reddy, David Cournapeau, Evgeni Burovski, et al. 2020. “SciPy 1.0: Fundamental Algorithms for Scientific Computing in Python.” Nature Methods 17 (3): 261–72.

Wang, B.; Yang,W.; Wen,W.; Sun, J.; Su, B.; Liu, B.; Ma, D.; Lv, D.;Wen, Y.; Qu, T.; et al. Gamma-secretase gene mutations in familial acne inversa. Science 2010, 330, 1065

Wang, Z.; Yan, Y.; Wang, B.; γ-Secretase Genetics of Hidradenitis Suppurativa: A Systematic Literature Review. Dermatology. 2020 Dec 17;1-7.

Wolfe, M.S.; Xia,W.; Ostaszewski, B.L.; Diehl, T.S.; Kimberly,W.T.; Selkoe, D.J. (1999) Two transmembrane aspartates in presenilin-1 required for presenilin endoproteolysis and gamma-secretase activity. Nature, 398, 513–517.

Wong, P.C.; Zheng, H.; Chen, H.; Becher, M.W.; Sirinathsinghji, D.J.; Trumbauer, M.E.; Chen, H.Y.; Price, D.L.; Van der Ploeg, L.H.; Sisodia, S.S. Presenilin 1 is required for Notch1 andDll1 expression in the paraxial mesoderm. Nature 1997, 387, 288–292.

Yang J, Wang L, Huang Y, Liu K, Lu C, Si N, Wang R, Liu Y, Zhang X. Keratin 5-Cre-driven deletion of Ncstn in an acne inversa-like mouse model leads to a markedly increased IL-36a and Sprr2 expression. Front Med. 2020 Jun;14(3):305-317.

Zoltowska KM, Das U, Lismont S, Enzlein T, Maesako M, Houser MCQ, Franco ML, Gomes MD, Karachentsev D, Becker A, Hopf C, Vilar M, Berezovska O, Mobley W, Chávez-Gutiérrez L. Alzheimer's disease linked Aβ42 exerts product feedback inhibition on γ-secretase impairing downstream cell signaling. bioRxiv [Preprint]. 2023 Aug 2:2023.08.02.551596.

Figure 1

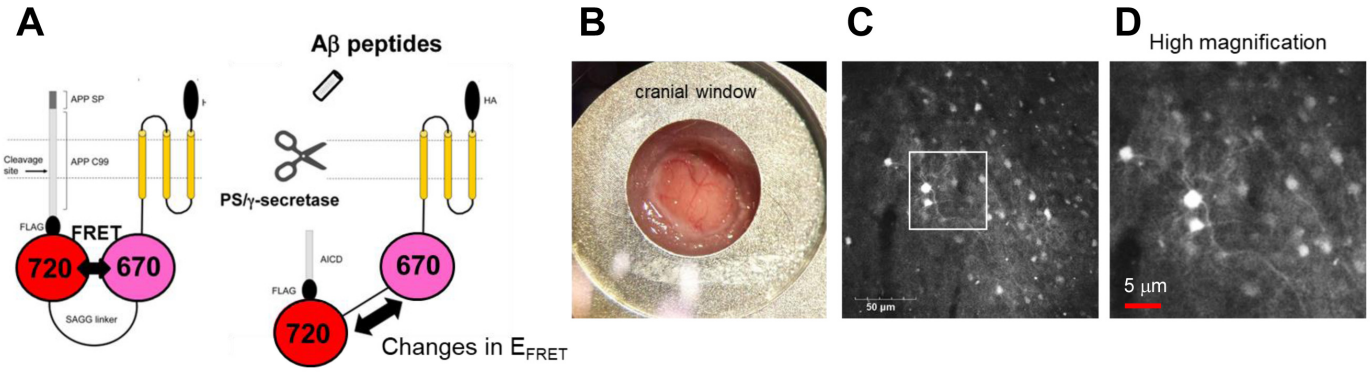

<u>Expression of the C99 720-670 biosensor in the living mouse brain</u> **(A)** A schematic presentation of the C99 720-670 biosensor. **(B)** A cranial window was implanted on the top of the brain for image acquisition. **(C)** Extensive expression of the C99 720-670 biosensor in the somatosensory cortex was verified by confocal microscopy *in vivo*. Scale bar: 50 µm. **(D)** A high magnification image corresponding to the square in Fig. 1C. Scale bar: 5 µm.

Figure 2

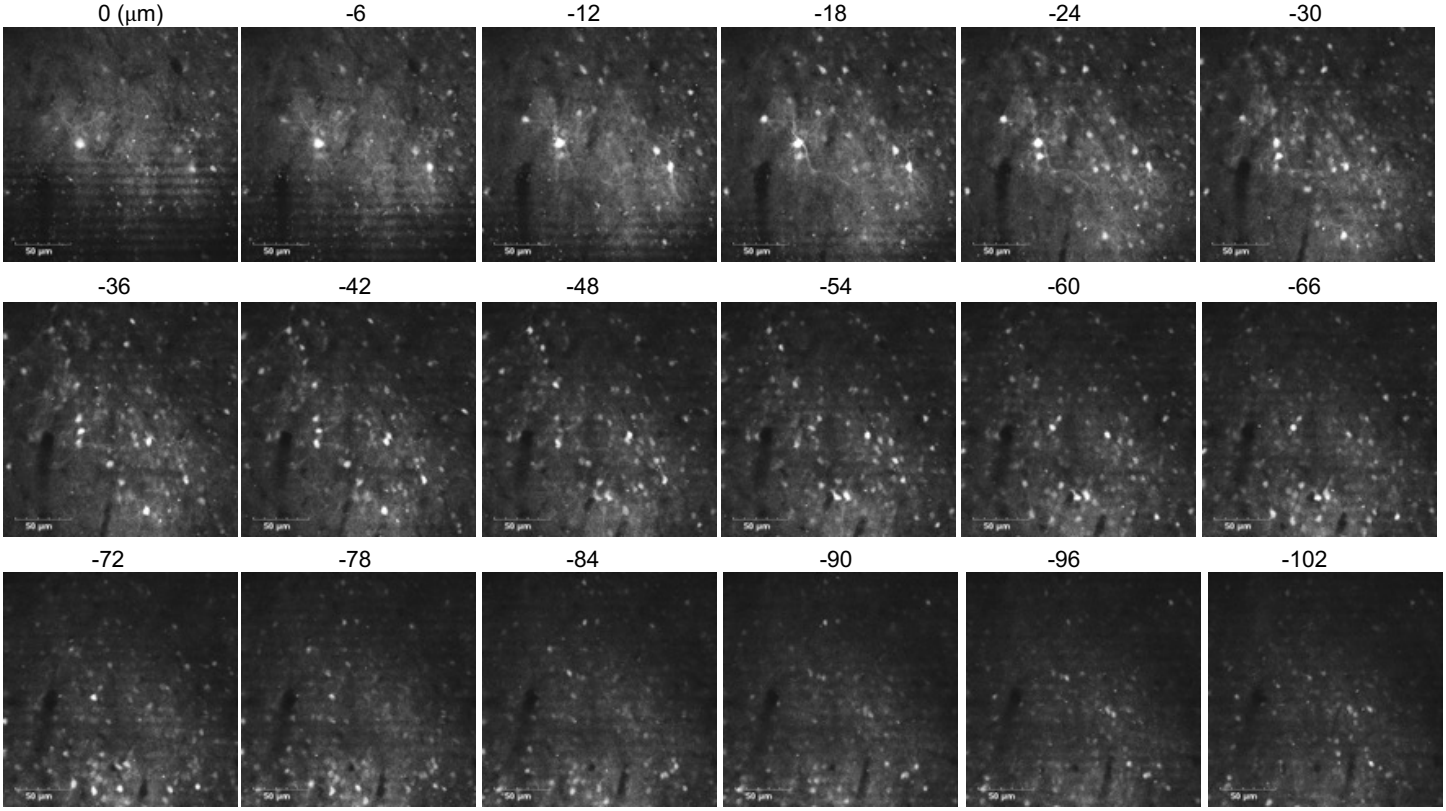

Z-section images of the brain expressing the C99 720-670 biosensor. The C99 720-670 biosensor fluorescence signal was detected at approximately 100 μm depth from the brain surface. Scale bar: 50 μm.

Figure 3

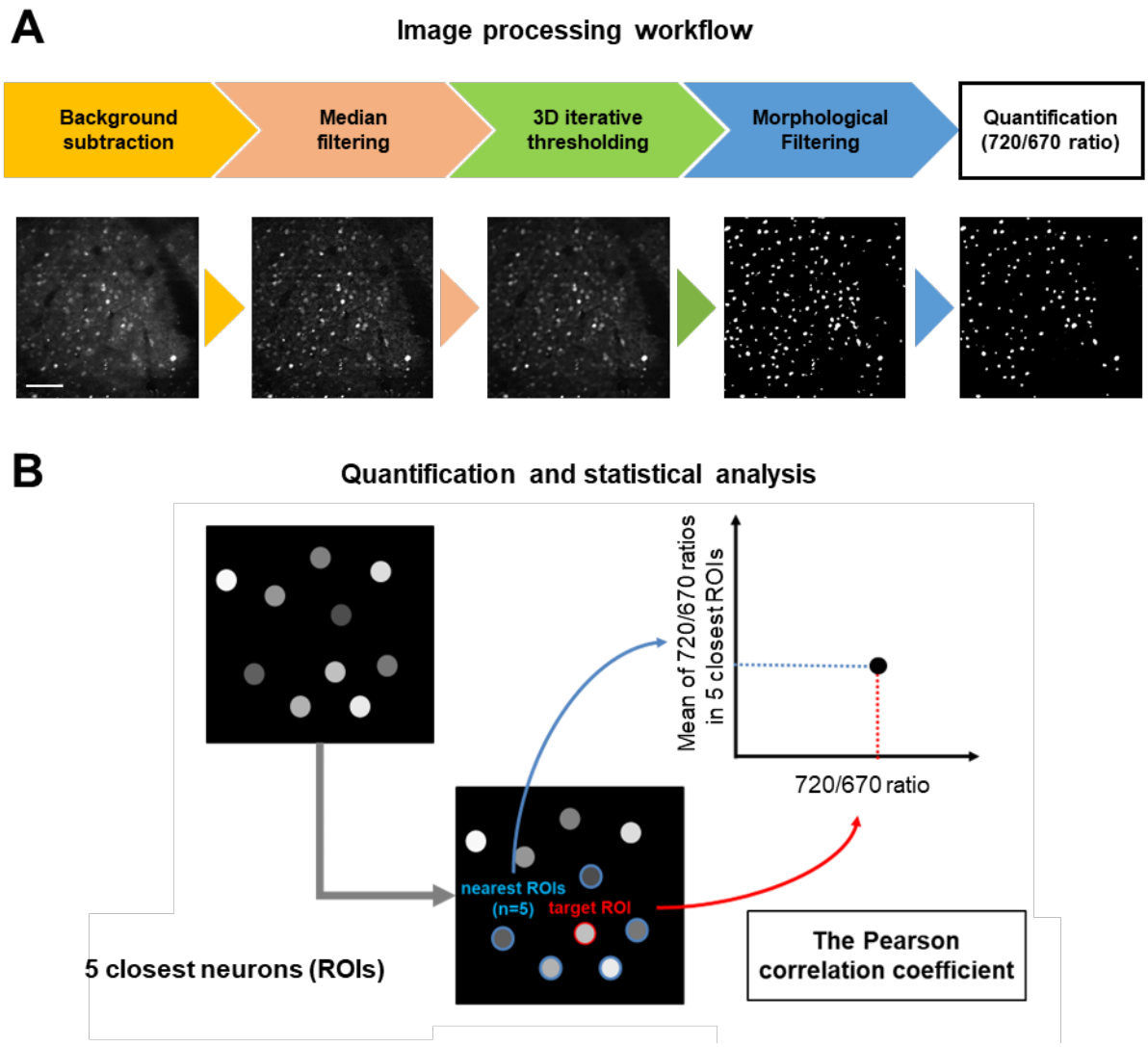

<u>Imaging processing workflow and data analysis</u> **(A)** Before measuring the acceptor over donor emission ratios (i.e., 720/670 ratios) on a cell-by-cell basis, which reports γ-secretase activity in individual neurons, four-step image processing steps were applied: 1) background subtraction, 2) median filtering, 3) 3D iterative thresholding, and 4) morphological filtering. Scale bar: 50 μm. **(B)** To elucidate the relationship between γ-secretase activity and those in neighboring neurons, the distance between neuron and neuron was first determined, then identified each neuron's five closest neurons, and calculated the average 720/670 ratio of the five neighboring neurons. The Pearson correlation coefficient between each neuron's 720/670 ratio and the average ratio of the five neighboring neurons was calculated.

Figure 4

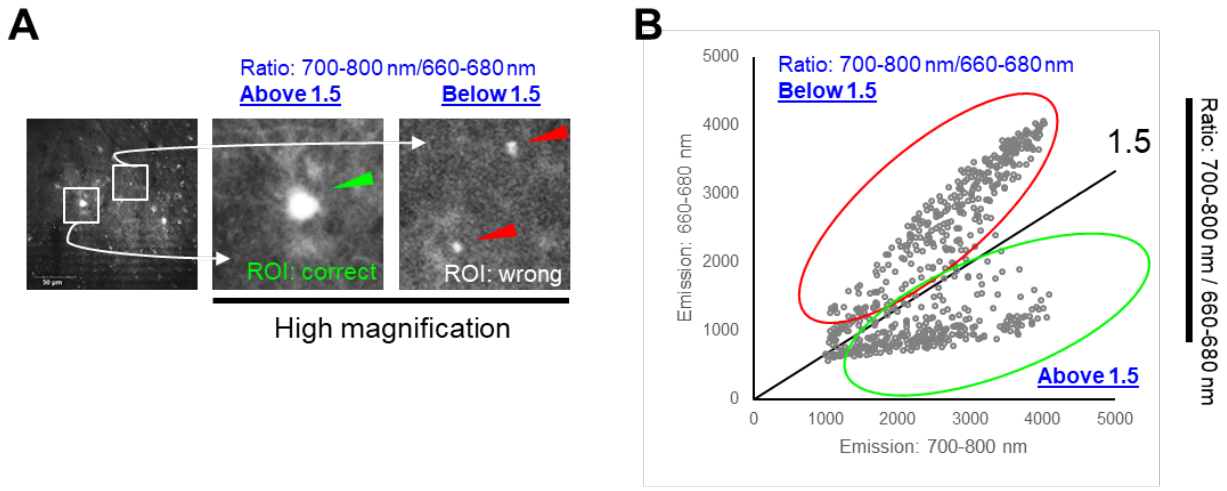

Identification and removal of auto fluorescent objects **(A)** Our four-step segmentation approach still could not perfectly remove wrongly assigned ROIs, such as shown in the right panel (red arrowheads). However, these ROIs displayed higher 660-680 nm emissions and thus significantly lower 720/670 ratios (below 1.5). **(B)** A scatter plot supported our observation**:** two populations of ROIs displaying 720/670 ratios above 1.5 and the ratios below, later of which were excluded from our data analysis.

Figure 5

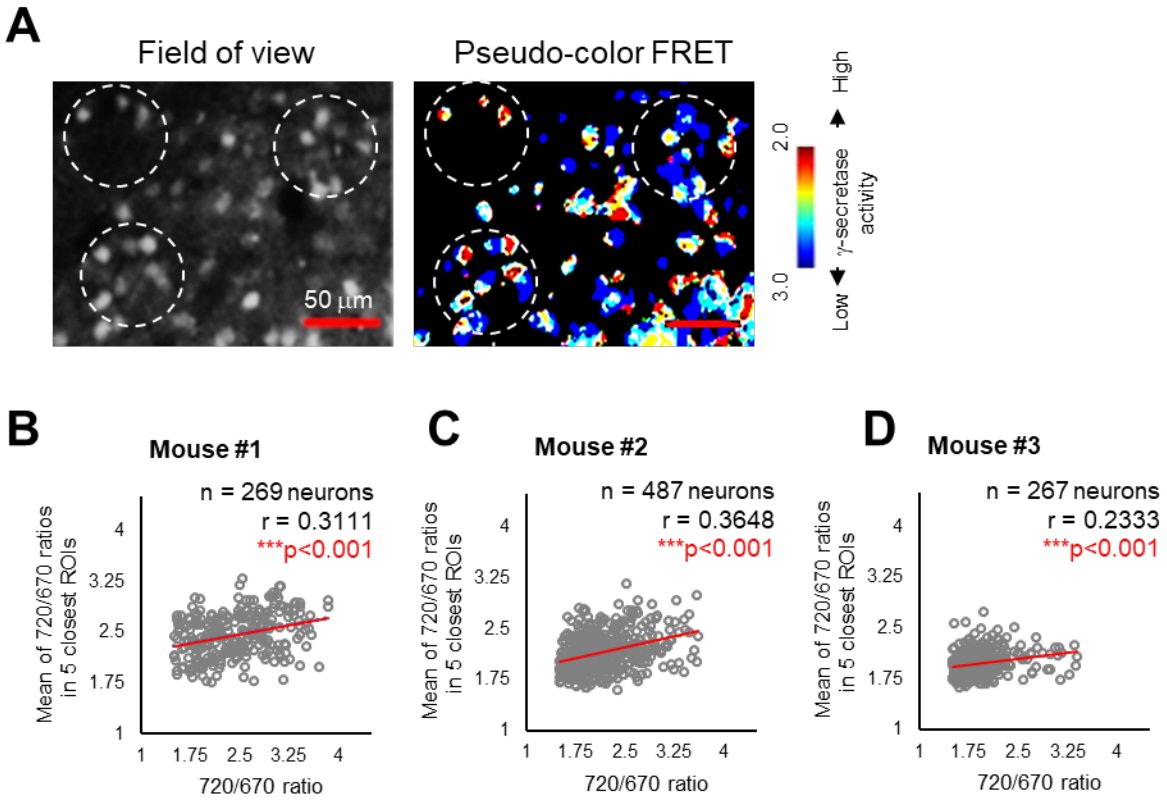

<u>A potential "cell non-autonomous" regulation of γ-secretase in mouse brains</u> **(A)** A representative image showing the expressions of the C99 720-670 biosensor (Field of view) and a pseudo-color image corresponding 720/670 ratios (Pseudo-color FRET). Scale bar: 50 μm. **(B-D)** Scatter plots showing the 720/670 ratio in individual neurons (X-axis) and the average Mean of the 720/670 ratio in five neighboring neurons in three independent mice. The number of neurons, correlation coefficient (r), and p-value are shown. Pearson correlation coefficient. *** $p < 0.001$

Figure 6

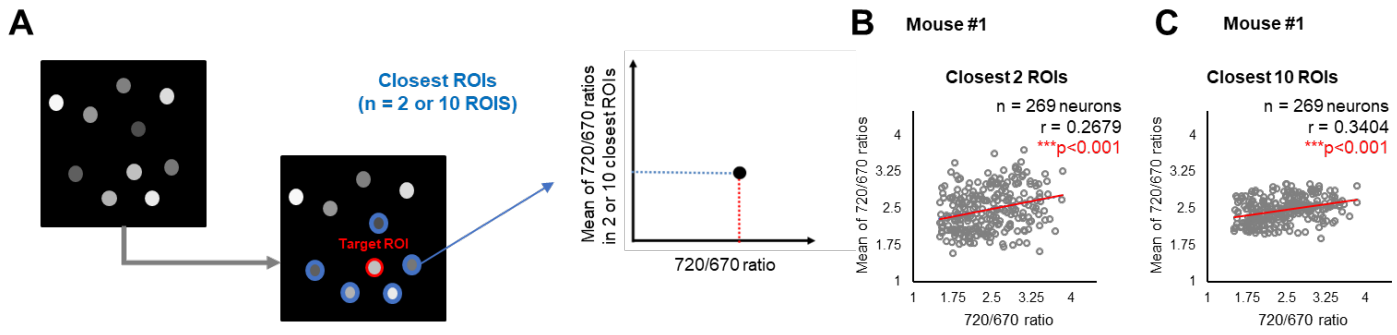

<u>Validation #1 - A potential "cell non-autonomous" regulation of γ-secretase in mouse brains</u> **(A)** The two or ten closest neurons were identified, and the average 720/670 ratio of the two or ten neighboring neurons was calculated and plotted. **(B)** We verified a significant positive correlation between the 720/670 ratio and the average ratio of two and **(C)** ten closest neurons. The number of neurons, correlation coefficient (r), and p-value are shown. Pearson correlation coefficient. *** $p < 0.001$

Figure 7

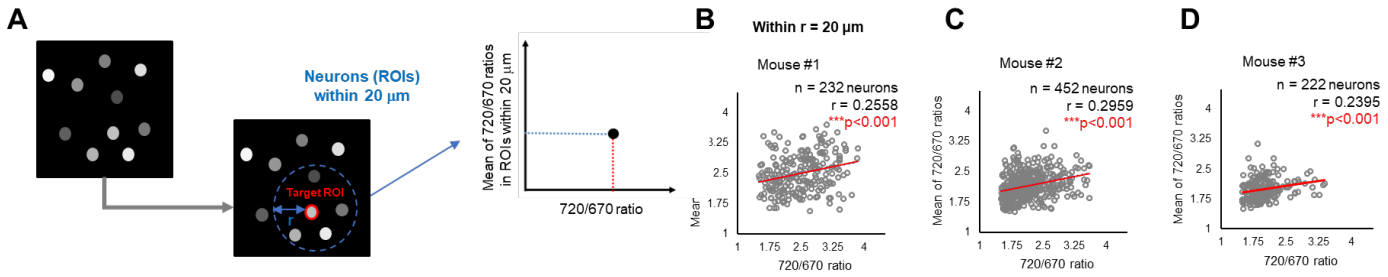

<u>Validation #2 - A potential "cell non-autonomous" regulation of γ-secretase in mouse brains</u> **(A)** The average 720/670 ratio of neurons within a 20 μm radius was calculated and plotted. **(B-D)** There was a significant positive correlation between the 720/670 ratio and the average ratio of neurons within a 20 μm radius in three independent mice. The number of neurons, correlation coefficient (r), and p-value are shown. Pearson correlation coefficient. *** $p < 0.001$

Figure 8

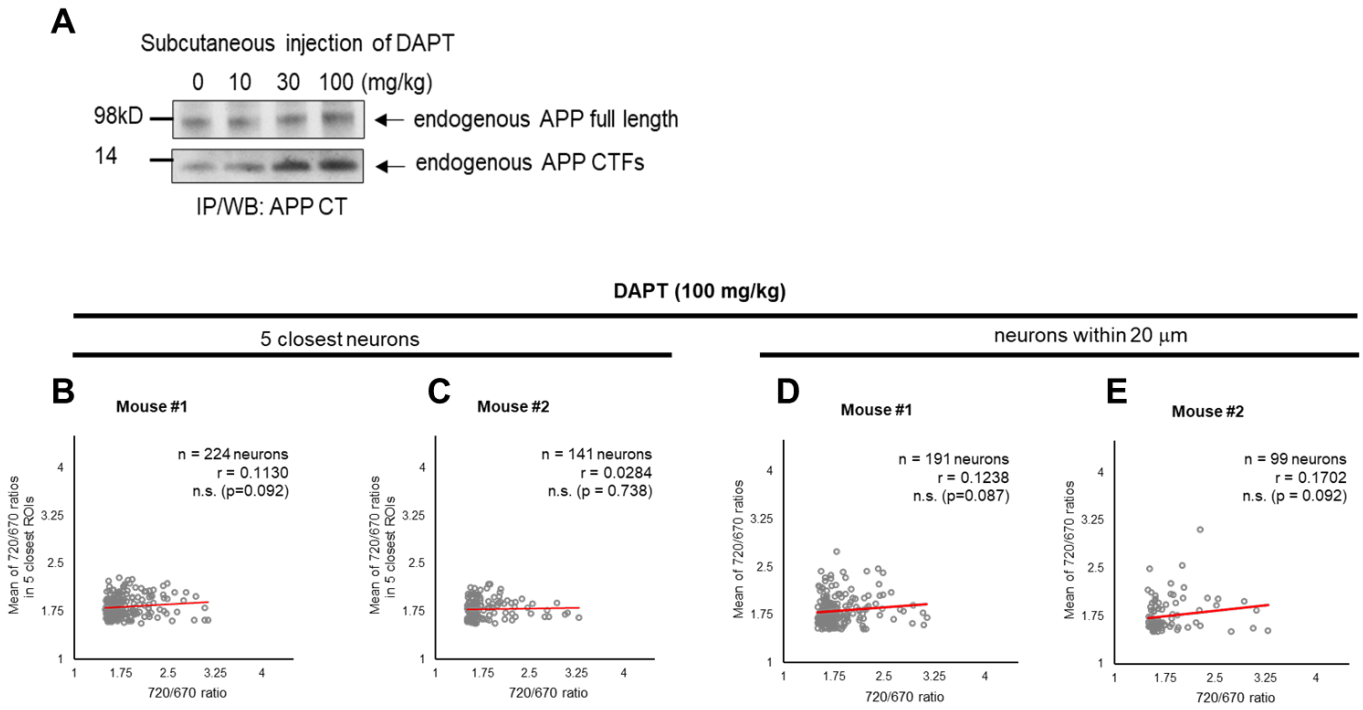

γ-Secretase inhibition cancels the "cell non-autonomous" regulation **(A)** The dose-dependent accumulation of endogenous APP C-terminus fragments (APP-CTFs) by subcutaneous administration of DAPT evidences the inhibition of γ-secretase activity in mouse brains. **(B** and **C)** Neither significant correlation between the 720/670 ratio and the average ratio of the five closest neurons, nor **(D** and **E)** the average ratio of neurons within a 20 μm radius. The number of neurons, correlation coefficient (r), and p-value are shown. Pearson correlation coefficient. n.s. not significant